

# Specific features of radiation emitted upon tunnel ionisation of atoms in extremely intense laser fields

S.V. Popruzhenko, E.B. Kalymbetov

**Abstract.** Radiation emitted by fast electrons in the process of multiple tunnel ionisation of heavy atoms in the focus of a laser pulse with extreme intensity exceeding  $10^{22}$  W cm $^{-2}$  is studied. It is shown that the spectral-angular distribution of emitted photons in a wide range of angles is qualitatively determined by relations of the synchrotron radiation theory. The dependences of the number and the characteristic frequency of emitted photons on the laser pulse parameters are estimated. The obtained results can be used to determine the maximum laser intensity in the focus.

**Keywords:** strong laser field, tunnel ionisation, synchrotron radiation, high-power lasers.

## 1. Introduction

At present, the study of the fundamental properties of electrodynamic effects in highly intense emission fields attracts increased interest. This is explained first of all by a significant progress achieved in recent years in the development of laser sources with record-high powers. The intensity and the absolute values of electric and magnetic field strengths are the key parameters of laser radiation and determine the character of its interaction with matter in nonlinear and ultrarelativistic regimes. Therefore, the upper limit of laser intensity achievable in laboratories to a large extent determines the possibility of experimental studies of classical and quantum dynamics of charged particles in strong external fields. The state of the art in this area of research, which develops at the confluence of nonlinear quantum electrodynamics, relativistic optics, and plasma physics, is reflected in reviews [1–3].

For a long time, peak powers in experiments on the physics of laser light interaction with atoms, electrons, and plasma have been limited by several hundreds of terawatts and, in exceptional cases, by a petawatt, which made it possible to achieve an intensity of  $5 \times 10^{21}$  W cm $^{-2}$  in the laser focus centre. There were only a few publications on achieving intensities of  $2 \times 10^{22}$  W cm $^{-2}$  [4]. In recent years, several laser systems of a multipetawatt power have been designed and fabricated [5–11]. These systems are expected to go into service soon

and to increase the peak intensities in a laser focus approximately by an order of magnitude, that is, to  $10^{23}$  W cm $^{-2}$ . The authors of recent paper [12] report on achieving, for the first time in the history of laser investigations, an intensity of  $10^{23}$  W cm $^{-2}$  from the CoReLS laser with a radiation power of 4 PW. Further development of the methods of adaptive optics and possible development of an exawatt laser within the XCELS project [13] allow one to hope to achieve electromagnetic pulses with intensities of  $10^{24}$  W cm $^{-2}$  and higher in the foreseeable future. It is expected that a considerable increase in the peak strength of electromagnetic fields available for experiments will make it possible to study new regimes of interaction of electromagnetic radiation with matter including the regime of dominated radiation friction in the dynamics of charged particles, generation of quantum electrodynamic cascades, excitation of ultrahigh magnetic fields in plasma, etc. [1–3].

Nonlinear ionisation of atoms and ions by intense laser radiation is one of the best studied effects in strong field physics. The current state of the theory and experiment on this effect is discussed in reviews [14–17] and references therein. Ionisation caused by the interaction of high-power laser pulses with gaseous and condensed media usually occurs at the initial stage, which itself is of no interest, and leads to the formation of plasma, whose further evolution under action of laser radiation is the main object of study. Nevertheless, the understanding of the ionisation process is important for determining the charge composition and other plasma characteristics. In addition, the observation of the tunnel ionisation of heavy atoms in the laser focus can be used to estimate the peak radiation intensity [18–23], which is important for correct description of observed effects and for experimental design. The plasma formed by ionisation serves as a source of secondary radiation, whose characteristics can be of interest for diagnostics of both the ionising laser pulse and the formed plasma. Finally, at intensities exceeding  $10^{24}$  W cm $^{-2}$ , electrons detached from atoms as a result of their multiple ionisation can cause the formation of quantum electrodynamic cascades [24, 25].

In the present work, we consider the radiation emitted in the process of electrons' detachment from heavy atoms in a rarefied gaseous target irradiated by a laser pulse with an intensity of about  $10^{22}$  W cm $^{-2}$ . The aim of this work is to qualitatively describe the spectral-angular energy distribution of this radiation and its dependence on the laser beam intensity and other characteristics. In particular, we will show that the spectral-angular distribution of radiation energy in the region of not very small and not very large angles with respect to the laser pulse propagation direction has a universal shape close to the shape for synchrotron radiation and the width of

---

**S.V. Popruzhenko** Prokhorov General Physics Institute, Russian Academy of Sciences, ul. Vavilova 38, 119991 Moscow, Russia; Institute of Applied Physics, Russian Academy of Sciences, 603950 Nizhny Novgorod, Russia; e-mail: sergey.popruzhenko@gmail.com;  
**E.B. Kalymbetov** National Research Nuclear University 'MEPhi', Kashirskoe sh. 31, 115409 Moscow, Russia

Received 9 July 2021

*Kvantovaya Elektronika* 51 (9) 801–806 (2021)

Translated by M.N. Basieva

---

the spectrum in this intermediate range of angles turns out to be proportional to the field strength in the laser focus centre.

## 2. Statement of the problem

In an intense field of laser radiation, multiple sequential detachments of electrons from atoms occur, which leads to the formation of ions with a high charge  $Z$ . The ionisation mechanism is determined by the Keldysh parameter [14, 26]

$$\gamma_K = \frac{\sqrt{2mI_p}\omega}{eE_0}, \quad (1)$$

where  $I_p$  is the ionisation potential of the atomic level,  $E_0$  is the electromagnetic wave field strength amplitude,  $\omega$  is the frequency of this wave, and  $e$  and  $m$  are the absolute electron charge and the electron mass, respectively. At  $\gamma_K \ll 1$ , ionisation occurs in the tunnelling regime in the same way as in a constant field. In this case, the ionisation probability per unit time is described by well-known formulae [14] applicable, in particular, in the case of the relativistic regime. For the considered problem of electron detachment from multicharged ions in the radiation field of an IR laser with a wavelength  $\lambda \approx 1 \mu\text{m}$  and an intensity of  $10^{22} \text{ W cm}^{-2}$  and higher, the Keldysh parameter is  $10^{-2} - 10^{-3}$  (see estimates in [21, 23]), that is, the tunnelling approximation is valid with a high accuracy and the tunnelling process occurs in the nonrelativistic regime. In the description of the emission of an electron appearing in a strong electromagnetic wave filed as a result of its detachment from an atom, the contribution of the tunnelling process itself is taken into account only in setting of the initial condition for the electron propagation in the wave field. In the case of tunnel ionisation, an electron is released from an atom with the zero velocity

$$\mathbf{v}(t_0, \mathbf{r}_0) = 0, \quad (2)$$

where  $\mathbf{r}_0$  is the radius vector determining the atom position and  $t_0$  is the electron release time. If the trajectory  $\mathbf{r}(t; t_0, \mathbf{r}_0)$  is found from the solution of the equation of motion

$$\frac{d\mathbf{p}}{dt} = e\mathbf{E} + \frac{e}{c}\mathbf{v} \times \mathbf{H} \quad (3)$$

( $\mathbf{p}$  is the electron momentum and  $\mathbf{E}$  and  $\mathbf{H}$  are the strengths of the electric and magnetic fields of the laser wave), then the spectral-angular distribution of radiation is determined by the classical electrodynamics formulae [27]

$$\mathbf{H}'(\Omega, \mathbf{n}) = \frac{ie\Omega}{c^2 R_0} \exp(iKR_0) \int_{t_0}^{\infty} \exp[i(\Omega t - \mathbf{K}\mathbf{r})] \mathbf{n} \times \mathbf{v} dt, \quad (4)$$

$$dW(\Omega, \mathbf{n}) = \frac{cR_0^2}{4\pi^2} |\mathbf{H}'(\Omega, \mathbf{n})|^2 d\Omega d\Omega, \quad (5)$$

where  $W$  is the radiation energy,  $d\Omega$  is the solid-angle element,  $\mathbf{n}$  is the unit vector in the radiation propagation direction,  $\mathbf{H}'$  is the vector of the magnetic field of radiation (do not confuse with the magnetic field vector  $\mathbf{H}$  of the laser wave),  $\Omega$  and  $\mathbf{K} = \Omega\mathbf{n}/c$  are its frequency and wave vector,  $R_0$  is the distance to the observation point, and  $\mathbf{v}(t) = \dot{\mathbf{r}}(t)$  is the electron velocity.

To describe the electromagnetic field of a laser wave, we will use the approximation of a linearly polarised Gaussian beam with the lowest TEM<sub>00</sub> mode,

$$\begin{aligned} \mathbf{E}(\mathbf{r}, t) &= \frac{E_0}{\sqrt{1 + z^2/z_R^2}} \\ &\times \exp\left\{-\frac{x^2 + y^2}{w_0^2(1 + z^2/z_R^2)} - i\left[\omega t - kz + k\frac{x^2 + y^2}{2R(z)} - \psi(z)\right]\right\}, \\ \mathbf{H}(\mathbf{r}, t) &= \mathbf{n}_0 \times \mathbf{E}. \end{aligned} \quad (6)$$

Here,  $w_0$  is the waist radius,  $z_R = \pi w_0^2/\lambda$  is the Rayleigh length,  $R(z) = z(1 + z^2/z_R^2)$  is the radius of the wavefront curvature,  $\psi(z) = \arctan(z/z_R)$  is the Gouy phase,  $\mathbf{n}_0$  is the unit vector in the beam propagation direction (along the  $z$  axis), and  $\mathbf{k} = 2\pi\mathbf{n}_0/\lambda$  is the wave vector. For numerical calculations, we use the following parameters:  $\lambda = 1 \mu\text{m}$ ,  $w_0 = 2 \mu\text{m}$ , and  $z_R \approx 12.6 \mu\text{m}$ ; in this case, the beam cross section in the focus at half maximum of the intensity distribution is  $d_0 = \sqrt{2 \ln 2} w_0 \approx 2.4 \mu\text{m}$  and the angular beam divergence is

$$\Theta = \arctan\left(\frac{\lambda}{\pi w_0}\right) \approx 0.16. \quad (7)$$

These parameters are close to those reported in [5] for SULF with a power of 10 PW. The electromagnetic field strength in the focal spot centre is characterised by the dimensionless parameter

$$a_0 = \frac{eE_0}{mc\omega}. \quad (8)$$

We will also use the notation  $a = a_0(\mathbf{r})$  for the  $\mathbf{r}$ -dependent parameter (8). To achieve the peak value  $a_0 = 10^2$ , which corresponds to the intensity  $I \approx 2 \times 10^{22} \text{ W cm}^{-2}$ , at the considered laser beam parameters, it is necessary to have a power of  $\sim 1.5 \text{ PW}$ , that is, an energy of  $\sim 50 \text{ J}$  at a pulse duration  $\tau = 30 \text{ fs}$ .

## 3. Main equations

### 3.1. Trajectories

To calculate the spectral-angular distribution of radiation energy, it is necessary to find the electron trajectory by solving Eqn (3). The trajectory for a Gaussian beam (6) can be found only numerically. Before considering the numerical calculation results, let us perform some estimates, which will allow us to qualitatively understand the electron motion character, using the uniform crossed field approximation, that is, assuming that

$$\mathbf{E} = \mathbf{E}(\mathbf{r}_0, \varphi_0), \quad \mathbf{H} = \mathbf{H}(\mathbf{r}_0, \varphi_0), \quad (9)$$

where  $\varphi_0 = \omega t_0 - \mathbf{k}\mathbf{r}_0$  is the phase of the laser wave field at the time of electron detachment from an atom located at the point  $\mathbf{r}_0$ . The applicability of the crossed field approximation can be justified as follows. The trajectory of an electron propagating with the zero initial velocity in a high-intensity electromagnetic field is strongly stretched in the pulse propaga-

tion direction, and the electron motion rapidly becomes ultra-relativistic. In the case of this copropagating motion, the field phase  $\varphi = \omega t - \mathbf{k}\mathbf{r}$  varies along the trajectory much more slowly than the dimensionless time  $\omega t$ , so that the electron leaves the strong field region for a proper time shorter than the laser wave period (see estimates below). We will assume that the electric field is polarised along the  $x$  axis. Then, the electron trajectory lies in the  $xz$  plane and the electron motion is described by the expressions

$$\begin{aligned} \tilde{x} &= \frac{a}{2}\varphi^2, \quad \tilde{z} = \frac{a^2}{6}\varphi^3, \quad p_x = mca\varphi, \quad p_z = \frac{mc}{2}a^2\varphi^2, \\ \varepsilon_{\text{kin}} &= mc^2\left(1 + \frac{a^2\varphi^2}{2}\right), \end{aligned} \quad (10)$$

where

$$\begin{aligned} \tilde{x} &= \frac{2\pi x}{\lambda}, \quad \tilde{z} = \frac{2\pi z}{\lambda}, \quad \varphi = \frac{2\pi s}{\lambda}, \text{ and} \\ s &= c \int_{t_0}^t dt \sqrt{1 - v^2/c^2} \end{aligned} \quad (11)$$

are the dimensionless variables;  $p_x$  and  $p_z$  are the transverse and longitudinal momentum components; and  $\varepsilon_{\text{kin}}$  is the electron kinetic energy.

Formulae (10) and (11) make it possible to estimate the time of electron presence in the laser focus. The final point of this time is determined by the time of electron escape from the strong field region through the side surface of the focal region, or through the pulse trailing edge due to a phase lag, or due to the electron motion together with the laser pulse to the region in which the Gaussian beam is already defocused. For estimates, let us consider a trajectory beginning in the focal spot centre at the time when the field is maximum ( $r_0 = 0$ ,  $\varphi_0 = 0$ ). We will assume that an electron escapes through the side surface of the focal region if its coordinate is  $x = bw_0$ , where  $b$  is a numerical coefficient of the order of unity. Then, the field phase corresponding to the escape time is

$$\delta\varphi_x = 2\sqrt{\frac{b}{\Theta a_0}}. \quad (12)$$

The phase at which an electron propagating along the  $z$  axis enters the region of the weak field (with the same strength as in the previous estimate) is

$$\delta\varphi_z = \left(\frac{12e^{b^2}}{\Theta^2 a_0^2}\right)^{1/3}. \quad (13)$$

Finally, the phase at which an electron escapes the high-intensity region through the trailing edge of the laser pulse with duration  $\tau$  is determined from the condition  $ct(\delta\varphi_\tau) - z(\delta\varphi_\tau) \approx c\tau$  as

$$\delta\varphi_\tau = \omega\tau. \quad (14)$$

It is obvious that, at  $a_0 \gg 1$ , inequalities  $\delta\varphi_\tau \gg \delta\varphi_x, \delta\varphi_z$  are fulfilled, which justifies the constant field approximation. Let us estimate the relation between phases (12) and (13). For  $b = 2$ , we have

$$\frac{\delta\varphi_x}{\delta\varphi_z} \approx 0.33(\Theta a_0)^{1/6}. \quad (15)$$

This estimate shows that phases (12) and (13) are close to each other in a wide range of parameters, because of which each of them can be used for approximate calculation of the effective time of electron presence in the focus. The electron escape from the high-intensity region occurs mainly due to its motion along the  $z$  axis only in a very strong field and at strong focusing. The characteristic values of phases (12) and (13) for  $a_0 = 10^2$  are  $\delta\varphi_x \approx 0.5$  and  $\delta\varphi_z \approx 0.9$ . These values are small in comparison with  $2\pi$  but are considerable in comparison with unity. Thus, the crossed field approximation can be used, strictly speaking, only for qualitative estimates. Nevertheless, as is seen from the results given below, in some cases it is also applicable for quantitative consideration.

Figure 1 shows the electron trajectories obtained in the crossed field approximation and by the exact numerical solution of Eqn (3) in field (6) for several values of  $r_0$  inside the focal region. In all cases, it was assumed that an electron is detached from an atom at the time when  $\varphi_0 = 0$ , that is, when the electric field is maximum and directed counter to the  $x$  axis. One can see that the crossed field approximation is generally valid and, in the initial trajectory segment, which lies in the region of the maximum intensity and, therefore, makes the maximum contribution to radiation, the exact and approximate trajectories almost coincide. An important role in the description of radiation characteristics is played by the electron velocity direction, which makes the following angle with the  $z$  axis:

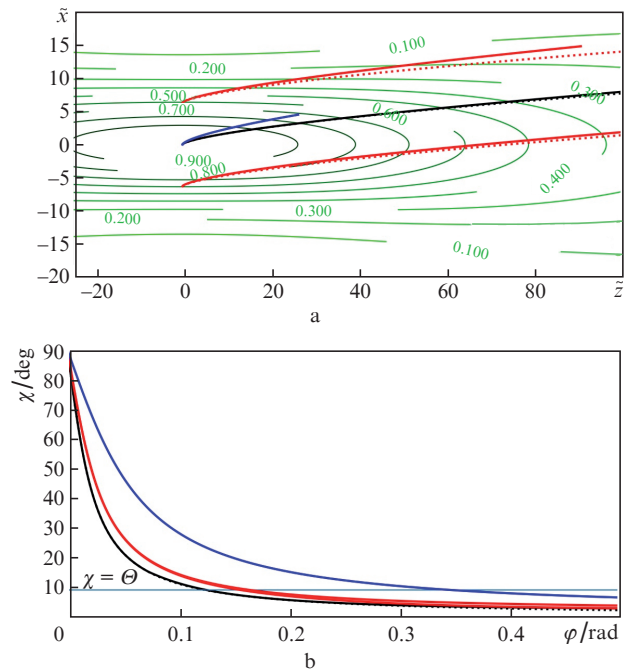


**Figure 1.** (Colour online) (a) Electron trajectories in the plane of dimensionless parameters  $\tilde{x}$   $\tilde{z}$  found (solid curves) numerically from Eqn (3) and (dashed curves) by formulae (10) for initial points with coordinates (black curves)  $x_0 = y_0 = z_0 = 0$ , (red curves)  $x_0 = \pm 1 \mu\text{m}$ ,  $y_0 = z_0 = 0$ , and (blue curves)  $y_0 = 2 \mu\text{m}$ ,  $x_0 = z_0 = 0$ , as well as isolines of the Gaussian beam intensity (6). (b) Dependences of the angle of inclination  $\chi$  (16) on the phase  $\varphi$  for the same trajectories.

$$\chi = \arctan \frac{p_x}{p_z} = \arctan \frac{2}{a\varphi}. \quad (16)$$

The phase at which the velocity direction falls into the solid angle formed by the laser beam cone is

$$\delta\varphi_\Theta = \frac{2}{a_0\Theta}, \quad (17)$$

and turns out to be rather small, namely, at the considered parameters for the trajectory beginning in the focal spot centre (Fig. 1b), it is  $\delta\varphi_\Theta \approx 0.1 \ll \delta\varphi_{x,z}$ .

### 3.2. Radiation

Next, let us study the characteristics of radiation emitted in the case of electron motion along the trajectories considered in the previous section. The crossed field approximation allows one to qualitatively estimate the spectral-angular distribution of emitted photons without calculating integral (4) along the  $\mathbf{r}(t)$  trajectory. The calculation based on approximate evaluation of this integral will be presented in a more detailed future work. For trajectory (10) in a crossed field, the closed analytical formulae for the spectral-angular distribution of radiation can be obtained in some special cases [28, 29], for example, for asymptotically free trajectories propagating through the field region. These results cannot be used for our problem due to the initial condition according to which the trajectory starts inside the focal region rather than outside it.

According to (10), the electron motion becomes relativistic at

$$\varphi - \varphi_0 \equiv \delta\varphi' = \frac{1}{a_0} \ll \delta\varphi_\Theta \ll \delta\varphi_{x,z}, \quad (18)$$

that is, long before the electron escapes the focus. Thus, the electron motion along the most part of the trajectory in the strong field region is ultrarelativistic. Since the longitudinal momentum in this case increases faster than the transverse one [see formula (10)], the electron motion rapidly becomes concurrent, which, as is known, leads to strong suppression of quantum effects even at very high  $a_0$ . Therefore, to describe the radiation characteristics, we can use the classical electrodynamics formulae, in particular, their ultrarelativistic asymptotics. Further simplification is possible by taking into account that, throughout most of the trajectory, the angle of its inclination considerably exceeds the angle corresponding to the effective width of the radiation cone [27]

$$\delta\theta \approx \frac{1}{\gamma} \approx \frac{1}{1 + a_0^2\varphi^2/2}, \quad (19)$$

which becomes small  $\delta\varphi_\Theta > \varphi \gg 1/a_0$ . In (19),  $\gamma$  is the relativistic factor and  $\theta$  is the angle that determines the radiation propagation direction ( $\cos\theta = \mathbf{nn}_0$ ). In the angular range  $\chi_0 > \theta \gg \delta\theta$  (Fig. 1b), radiation can be described in the synchrotron approximation [27] taking into account that the radiation at each time instant  $t$  is directed along the  $\mathbf{v}(t)$  vector, that is,  $\theta \approx \chi$ . Here,  $\chi_0$  is the angle corresponding to the phase at which the motion becomes ultrarelativistic. If the ultrarelativistic range boundary is taken to be  $\gamma = 10$ , then, for  $a_0 =$

$10^2$ , we have  $\chi_0 = 0.44 = 25^\circ$ . The total radiation power in the crossed field approximation remains constant, which contradicts the physical statement of the problem because the electron rather quickly escapes the strong field region. As seen from the shape of trajectories shown in Fig. 1, the electron escape from the strong field region occurs at  $\varphi \approx 0.2-0.4$ . Under these conditions, a reasonable approximation for calculating the power is its evaluation along the trajectory obtained in the case of the crossed field by the formula [27]

$$P = \frac{2e^4}{3m^2c^3} \frac{(\mathbf{E} + \mathbf{v} \times \mathbf{H}/c)^2 - (\mathbf{vE})^2/c^2}{1 - \mathbf{v}^2/c^2}, \quad (20)$$

using the exact values of  $\mathbf{E}$  and  $\mathbf{H}$ . Figure 2 shows dependences  $P(\varphi)$  calculated by formula (20) for trajectories found in the crossed field approximation and numerically calculated from Eqn (3) for field (6).

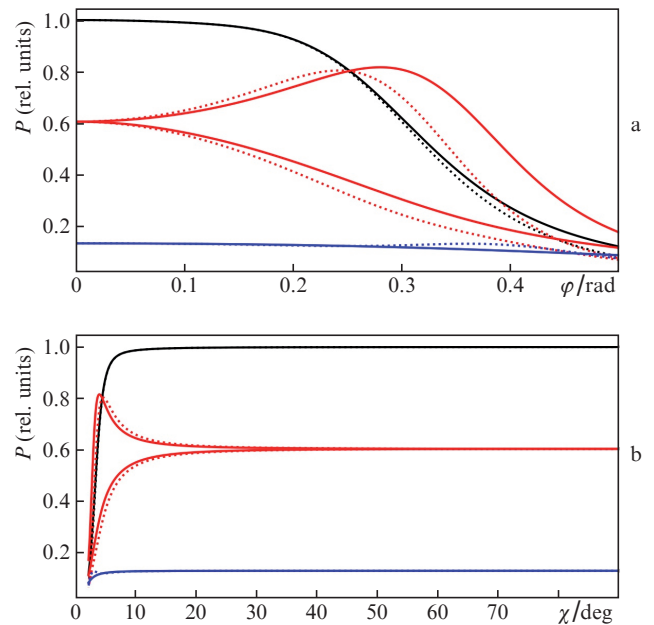


**Figure 2.** (Colour online) (a) Dependences of radiation power  $P$  on phase  $\varphi$  calculated by formula (20) along the trajectories found (solid curves) numerically from Eqn (3) and (dashed curves) in the crossed field approximation for the Gaussian beam field (6); (b) dependences of power  $P$  on the trajectory inclination angle  $\chi$ . The initial conditions are the same as for Fig. 1. The power for trajectories starting from point  $x_0 = -1 \mu\text{m}$  is higher than for trajectories starting from  $x_0 = +1 \mu\text{m}$ . The power is normalised to  $P(\varphi = 0)$  at point  $\mathbf{r} = 0$ , where the Gaussian beam field is maximum.

Taking into account that, in the case of ultrarelativistic motion in the range  $\theta \gg \delta\theta$ , acceleration  $\dot{\mathbf{v}}$  is almost orthogonal to the velocity, the qualitative form of the angular distribution can be easily determined using the formula [27]

$$dP = \frac{e^2 \dot{\mathbf{v}}^2}{4\pi c^3} \frac{d\Omega}{\left[1 - \frac{v \cos(\theta - \chi)}{c}\right]^4}. \quad (21)$$

To calculate energy  $dW$  emitted in solid angle  $d\Omega$ , it is necessary to integrate (21) over time. Omitting the calculation details, we present the approximate result for the case of the crossed field in the form



$$\frac{dW}{d\theta} = \frac{3a_0 e^2 \omega}{2c} \left(1 + \frac{a_0^2 \varphi_*^2}{2}\right) \left(1 + \frac{a_0^2 \varphi_*^2}{4}\right) \left(1 + \frac{a_0^4 \varphi_*^4}{4}\right), \quad (22)$$

where  $\varphi_* = 2/(a_0 \tan \theta)$ . Function (22) sharply increases in the region of small angles, as it should be in a crossed field, where the velocity asymptotically becomes codirected with the  $z$  axis. If we use in (21) a precise trajectory taking into account the electron escape from the focus, then the angular distribution will be stretched forward as before but remained everywhere finite.

The spectrum of emitted photons can also be qualitatively described without exact calculation of integral (4) keeping in mind that, in the wide range of angles  $\pi/2 > \theta \gg \delta\theta$ , radiation in the given direction is formed on a small trajectory segment that can be considered as a circle with the instantaneous radius of curvature  $\rho(\varphi)$  and angular velocity

$$\omega_{\text{eff}}(\varphi) \approx \frac{c}{\rho(\varphi)}. \quad (23)$$

In this approximation, electrons' emission is equivalent to synchrotron radiation in the magnetic field

$$H_{\text{eff}} = \frac{mc\omega_{\text{eff}}\gamma}{e}, \quad (24)$$

and the spectrum in the given direction can be found using well-known formulae (see, for example, § 73 in [27]), in which the magnetic field strength has the form of (24) and the harmonic number  $n = \Omega/\omega_{\text{eff}}$  is considered as a continuous parameter. Let us estimate the characteristic frequency  $\Omega$  in the emission spectrum as a function of angle  $\theta$  using the well-known relation [27]

$$\Omega_* = \frac{eH}{mc} \gamma^2. \quad (25)$$

In the crossed field approximation,

$$\Omega_* = \omega a_0 \sqrt{1 + \frac{a_0^4 \varphi_*^4}{4}}. \quad (26)$$

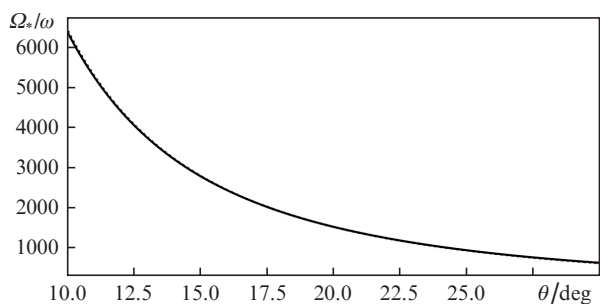


**Figure 3.** Dependences of the characteristic frequency (25) normalised to the laser wave frequency on the radiation propagation direction. The solid curve shows the result found using exact trajectories and the dashed curve corresponds to the result obtained in the crossed field approximation by formula (26). The exact and approximate results almost coincide.

In the range of angles  $\theta \approx \Theta$ , this estimate yields  $\Omega_* \approx 2\omega a_0/\Theta^2$ . Figure 3 shows the ratios  $\Omega_*/\omega$  obtained by formula (26) and by the exact numerical solution of equations of motion in the range of angles  $10^\circ - 30^\circ$ , which approximately coincides with the range  $[\Theta, \chi_0]$ . One can see that the exact and approximate results almost coincide.

## 4. Conclusions

The results presented in this work make it possible to qualitatively describe the main specific features of the spectral-angular distributions of radiation emitted upon tunnelling ionisation of atoms by laser pulses of ultrahigh intensities. The main distinction of the presented formulae for trajectories and spectra from the previously known formulae for the cases of a crossed field [28, 29] and a plane electromagnetic wave [30] is related to the initial condition (2) for motion of an electron appearing in the strong field region with a zero velocity. Our results also significantly complement the results of work [31], the authors of which considered the electron motion and emission in the field of a focused laser pulse but did not discuss the spectral-angular radiation characteristics, while the approximation for the wave electric field in [31] was even rougher than the Gaussian-beam approximation (6) used in the present work.

The role played by the field focusing in the radiation formation is significant because it is responsible for the limited values of the interaction time determined by formulae (12) and (13) and for the finite radiation power in the direction of the laser wave propagation. Comparison of the trajectories and emission characteristics obtained by numerical solution of the equations of motion and in the crossed field approximation shows that the latter is applicable with a rather high accuracy. This circumstance will considerably simplify the calculation of radiation parameters in a realistic experimental situation, description of which requires calculation of a large number of trajectories corresponding to the initial points with coordinates  $r_0, \varphi_0$  and to the fields in them. The characteristic frequencies (26) in the emission spectra depend on the laser wave field amplitude, which provides the principal possibility of estimating the laser radiation intensity in the focus by the shape of the spectrum.

An important feature of the considered case is the relatively low radiation power, which is linearly proportional to the intensity in the focal spot of the laser pulse, that is,  $P \propto a_0^2$ , while the radiation power in the case of electron motion in the field of a strong electromagnetic wave with a zero average velocity quadratically increases with increasing intensity,  $P \propto a_0^4$  [27, 30]. As a result, the total energy emitted by an electron for the time spent to its escape from the focal plane,

$$W \approx P(0)\delta t = P(0) \frac{dt}{d\varphi} \delta\varphi_{x,z}, \quad P(0) = \frac{2e^2 \omega^2 a_0^2}{3c} \quad (27)$$

is also low for our parameters, namely,  $W \approx 10^3 - 10^4$  eV. Taking into account that the characteristic energy of an emitted photon is estimated from (26) and Fig. 3 to be also  $10^3 - 10^4$  eV, we come to the conclusion that the average number of photons emitted by one electron is low, because of which experimental observation of emission can be very difficult. The requirements to experimental diagnostics necessary for recording emission under these conditions will be considered in detail in a future publication.

**Acknowledgements.** The authors thank I.Yu. Kostyukov, A.A. Mironov, and A.M. Fedotov for useful discussions. This work was supported by the Russian Science Foundation (Grant No.20-12-00077).

## References

1. Mourou G., Tajima T., Bulanov S.V. *Rev. Mod. Phys.*, **78**, 309 (2006).
2. Di Piazza A., Müller C., Hatsagortsyan C.Z., Keitel C.H. *Rev. Mod. Phys.*, **84**, 1177 (2012).
3. Narozhny N.B., Fedotov A.M. *Contemp. Phys.*, **56**, 249 (2015).
4. Yanovsky V. et al. *Opt. Express*, **16**, 2109 (2008).
5. Guo Z. et al. *Opt. Express*, **26**, 26776 (2018).
6. Papadopoulos D. et al. *High Power Laser Sci. Eng.*, **4**, e34 (2016).
7. Sung J.H. et al. *Opt. Lett.*, **42**, 2058 (2017).
8. Zeng X. et al. *Opt. Lett.*, **42**, 2014 (2017).
9. Gan Z. et al. *Opt. Express*, **25**, 5169 (2017); Li W. et al. *Opt. Lett.*, **43**, 5681 (2018).
10. Chambaret J.-P. et al. *Proc. SPIE*, **7721**, 77211D (2010).
11. Weber S. et al. *Mater. Radiat. Extremes*, **2**, 149 (2017).
12. Yoon J.W. et al. *Optica*, **8**, 630 (2021).
13. Bashinov A.V., Gonoskov A.A., Kim A.V., Mourou G., Sergeev A.M. *Eur. Phys. J. Spec. Top.*, **223**, 1105 (2014).
14. Popov V.S. *Phys. Usp.*, **47**, 855 (2004) [*Usp. Fiz. Nauk*, **174**, 921 (2004)].
15. Milosevic D.B., Paulus G.G., Bauer D., Becker W. *J. Phys. B: At. Mol. Opt. Phys.*, **39**, R203 (2006).
16. Popruzhenko S.V. *J. Phys. B: At. Mol. Opt. Phys.*, **47**, 204001 (2014).
17. Karnakov B.M., Mur V.D., Popruzhenko S.V., Popov V.S. *Phys. Usp.*, **58**, 3 (2015) [*Usp. Fiz. Nauk*, **185**, 3 (2015)].
18. Chowdhury C.A., Barty C.P.J., Walker B.C. *Phys. Rev. A*, **63**, 042712 (2001).
19. Yamakawa K., Akahane Y., Fukuda Y., Aoyama M., Inoue N., Ueda H. *Phys. Rev. A*, **68**, 065403 (2003).
20. Link A. et al. *Rev. Sci. Instrum.*, **77**, 10E723 (2006).
21. Ciappina M.F., Popruzhenko S.V., Bulanov S.V., Ditmire T., Korn G., Weber S. *Phys. Rev. A*, **99**, 043405 (2019).
22. Ciappina M.F., Popruzhenko S.V. *Laser Phys. Lett.*, **17**, 025301 (2020).
23. Ciappina M.F., Peganov E.E., Popruzhenko S.V. *Matter Radiat. Extremes*, **5**, 044401 (2020).
24. Tamburini M., Di Piazza A., Keitel C.H. *Sci. Rep.*, **7**, 5694 (2017).
25. Artemenko I.I., Kostyukov I.Yu. *Phys. Rev. A*, **96**, 032106 (2017).
26. Keldysh L.V. *Sov. J. Exp. Theor. Phys.*, **20**, 1307 (1965) [*Zh. Eksp. Teor. Fiz.*, **47**, 1945 (1964)].
27. Landau L.D., Lifshits E.M. *The Classical Theory of Fields* (London: Butterworth-Heinemann, 1980; Moscow: Nauka, 1988).
28. Ritus V.I. *J. Sov. Laser Res.*, **6**, 497 (1985).
29. Baier V.N., Katkov V.M., Strakhovenko V.M. *J. Exp. Theor. Phys.*, **73**, 945 (1991) [*Zh. Eksp. Teor. Fiz.*, **100**, 1713 (1991)].
30. Sarachik E.S., Schappert G.T. *Phys. Rev. D*, **1**, 2738 (1970).
31. Galkin A.L., Korobkin V.V., Romanovskii M.Yu., Shiryaev O.B. *Quantum Electron.*, **37**, 903 (2007) [*Kvantovaya Elektron.*, **37**, 903 (2007)].